STRUCTURAL SCIENCE
CRYSTAL ENGINEERING
MATERIALS

Volume 76 (2020)

Supporting information for article:

The order-disorder transition in Cu2Se and medium range ordering in the high temperature phase

Ping Lu, Wujie Qiu, Yuyu Wei, Chenxi Zhu, Xun Shi, Lidong Chen and Fangfang Xu

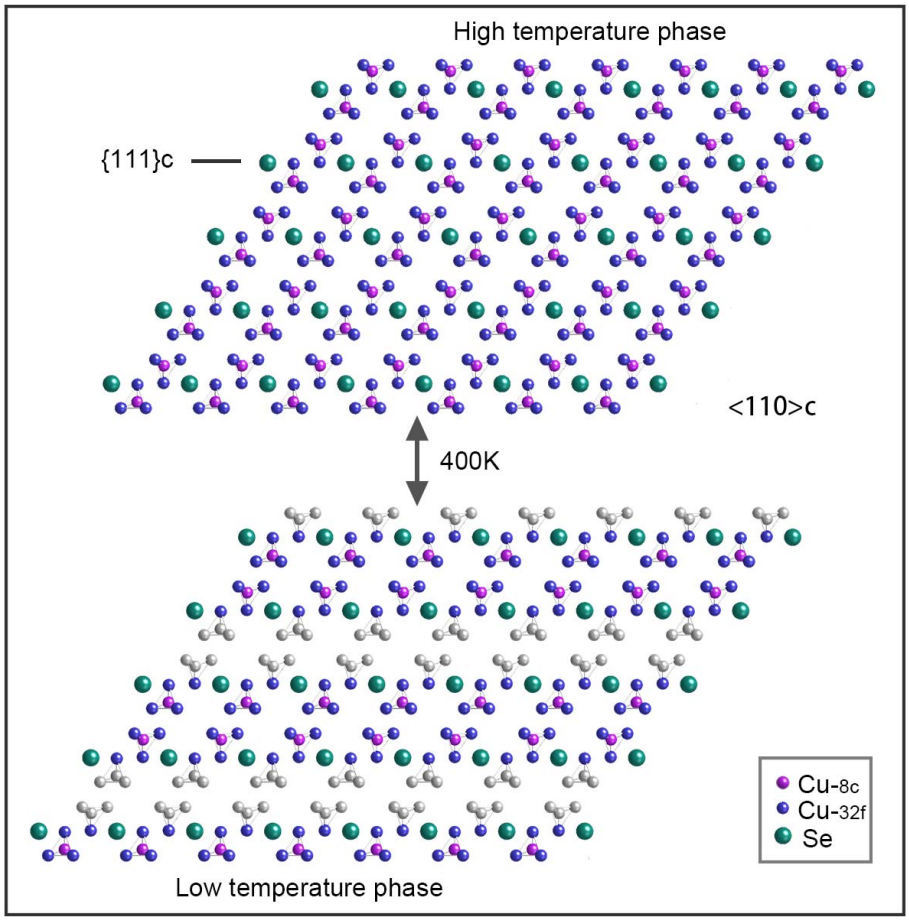

Fig. S1: Structural models for the disorder-to-order phase transition of Cu_2Se: Cu^+ ions which randomly occupy 8c and 32f sites in high temperature phase alternately gather into $\{111\}_c$ Se planes forming different ordered structures. Atoms in grey represent down to zero occupancy in their original interstitial 8c or 32f sites.

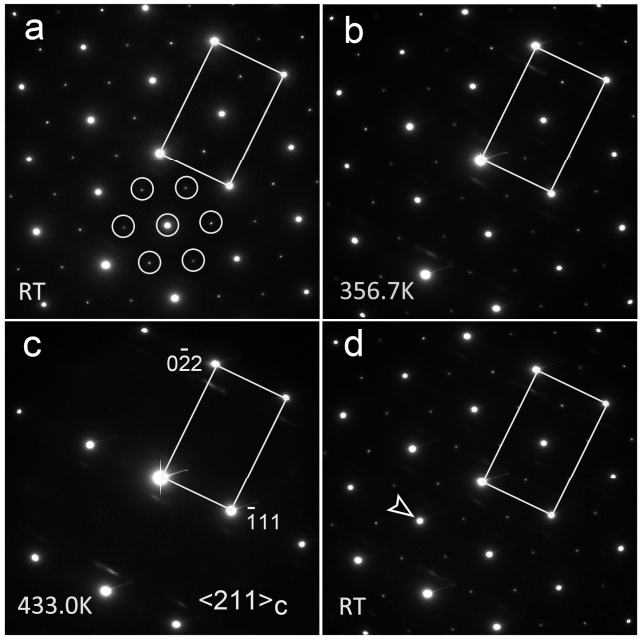

Fig. S2 In-situ electron diffraction analysis in a heating and cooling cycle. Here, the $<211>_c$ projection is the one other than parallel to the Cu-gathered interlayer thus shows different extra reflections (circled) from those in Fig. 1 in the text.

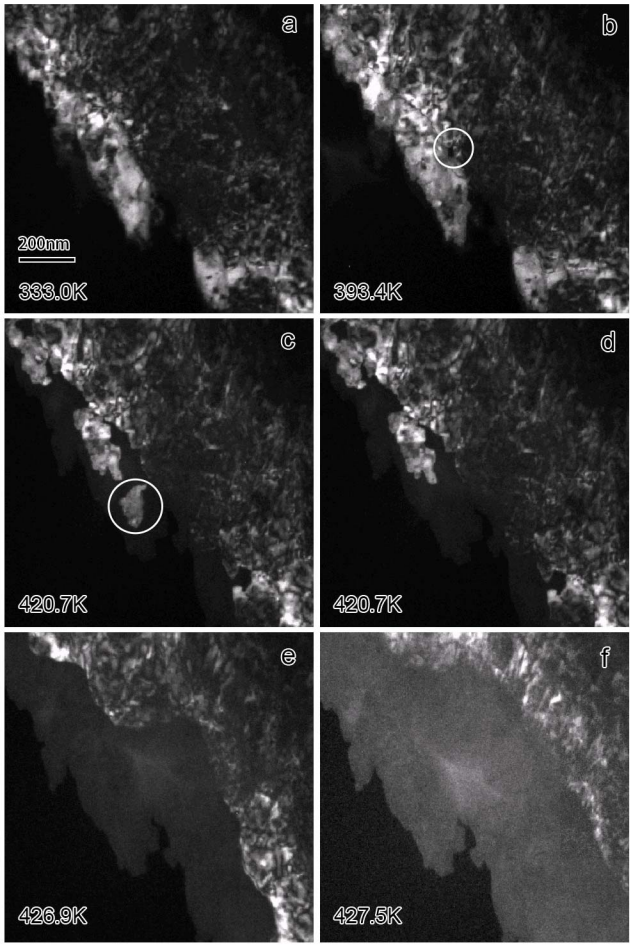

Fig. S3 In-situ dark-field (DF) imaging using the arrowed reflection in Fig. S2d. Thus the bright contrast in DF images represent the low temperature lamellar structure. The images are video captures at (a) 333.0 K, (b) 393.4 K, (c) 420.7 K, (d) 420.7 K, (e) 426.9 K, and (f) 427.5 K. Note the phase transition underwent in blocks of nanoscale in sudden while a nucleation process was absent.

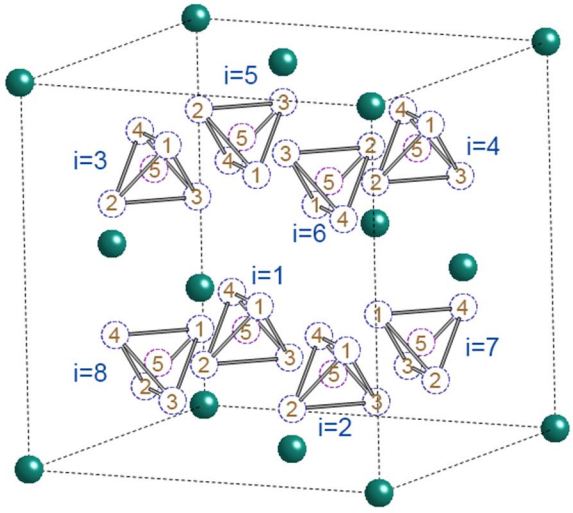

Figure S4: Indices of the 8c and 32f interstitial sites for Cu atoms in a cubic unit cell. There are eight sets of tetrahedral-arranged interstices in a unit cell, which are labeled as i=1, 2, 3… . Each tetrahedron consists of one 8c site (labeled as j=5) at the center and four 32f sites (labeled as j=1, 2, 3, and 4, respectively) at the corners.

Table S1: Coordinates of the Cu atoms in high-temperature Cu_2Se phase

i	j	x	y	z
1	1	0.334	0.334	0.334
1	2	0.334	0.166	0.166
1	3	0.166	0.334	0.166
1	4	0.166	0.166	0.334
1	5	0.250	0.250	0.250
2	1	0.834	0.834	0.334
2	2	0.834	0.666	0.166
2	3	0.666	0.834	0.166
2	4	0.666	0.666	0.334
2	5	0.750	0.750	0.250
3	1	0.834	0.334	0.834
3	2	0.834	0.166	0.666
3	3	0.666	0.334	0.666
3	4	0.666	0.166	0.834
3	5	0.750	0.250	0.750
4	1	0.334	0.834	0.834
4	2	0.334	0.666	0.666
4	3	0.166	0.834	0.666
4	4	0.166	0.666	0.834
4	5	0.250	0.750	0.750
5	1	0.334	0.334	0.666
5	2	0.334	0.166	0.834
5	3	0.166	0.334	0.834
5	4	0.166	0.166	0.666
5	5	0.250	0.250	0.750
6	1	0.666	0.666	0.666

6	2	0.666	0.834	0.834
6	3	0.834	0.666	0.834
6	4	0.834	0.834	0.666
6	5	0.750	0.750	0.750
7	1	0.334	0.666	0.334
7	2	0.334	0.834	0.166
7	3	0.166	0.666	0.166
7	4	0.166	0.834	0.334
7	5	0.250	0.750	0.250
8	1	0.666	0.334	0.334
8	2	0.666	0.166	0.166
8	3	0.834	0.334	0.166
8	4	0.834	0.166	0.334
8	5	0.750	0.250	0.250

Equation S1: (interference function)

$$I_s = \frac{sin^2\left(\frac{1}{2}N_1\vec{s}\cdot\vec{a}\right)}{sin^2\left(\frac{1}{2}\vec{s}\cdot\vec{a}\right)}\cdot\frac{sin^2\left(\frac{1}{2}N_2\vec{s}\cdot\vec{b}\right)}{sin^2\left(\frac{1}{2}\vec{s}\cdot\vec{b}\right)}\cdot\frac{sin^2\left(\frac{1}{2}N_3\vec{s}\cdot\vec{c}\right)}{sin^2\left(\frac{1}{2}\vec{s}\cdot\vec{c}\right)} \quad (\vec{s} = \vec{k} - \overrightarrow{k_0})$$

Equation S1 is inferred from the Debye scattering formula (Williams & Carter, 1996). In equation S1, $\vec{s} = 2\pi\overrightarrow{g_{hkl}} = 2\pi(h\vec{a}^* + k\vec{b}^* + l\vec{c}^*)$, $(\vec{a}, \vec{b}, \vec{c})$ are the basis vectors of the unit cell, $(\vec{a}^*, \vec{b}^*, \vec{c}^*)$ are the basis vectors of the reciprocal lattice. N1, N2, N3 are the repeatable numbers of the unit cell along the three basis vectors.

Equation S2: (structural factors of Cu sublattice)

$$F_{Cu-hkl} = f_{cu}\sum_{i=1}^{8}\sum_{j=1}^{5} O_{ij}e^{-i2\pi(hx_{ij}+ky_{ij}+ly_{ij})} \quad (O_{ij} = 1\ or\ 0)$$

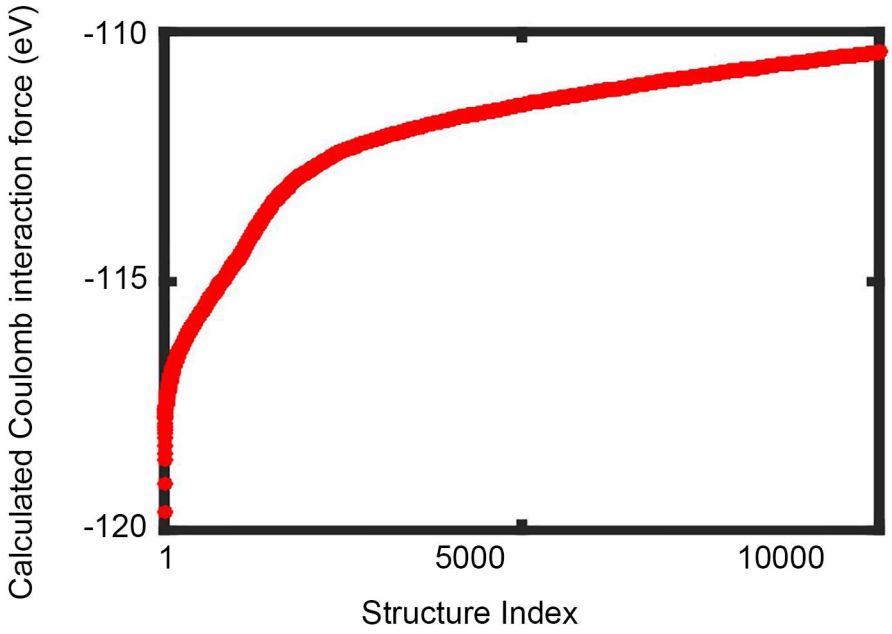

Figure S5: The energy curve of all possible structures calculated by Coulomb interaction methods.

Table S2: Arrangements of the Cu atoms in unit cells that fit the experimental results.

Structure Index Dx	Coordinates of Cu atoms		
D1	0.334	0.666	0.666
	0.666	0.334	0.334
	0.666	0.834	0.166
	0.334	0.166	0.834
	0.834	0.334	0.834
	0.166	0.666	0.166
	0.166	0.166	0.334
	0.834	0.834	0.666
D2	0.334	0.666	0.334
	0.666	0.334	0.334
	0.334	0.166	0.834
	0.666	0.834	0.834
	0.834	0.334	0.834
	0.166	0.666	0.834
	0.834	0.834	0.334
	0.166	0.166	0.334
D5	0.334	0.666	0.666
	0.666	0.334	0.334
	0.334	0.166	0.166
	0.666	0.834	0.834
	0.834	0.334	0.834
	0.166	0.666	0.166
	0.834	0.834	0.334
	0.166	0.166	0.666
D9	0.750	0.250	0.750
	0.250	0.750	0.750
	0.250	0.250	0.750

	0.750	0.750	0.750
	0.666	0.334	0.334
	0.666	0.834	0.166
	0.166	0.334	0.166
	0.166	0.834	0.334
D16	0.250	0.250	0.250
	0.750	0.750	0.250
	0.750	0.250	0.750
	0.250	0.750	0.750
	0.250	0.250	0.750
	0.750	0.750	0.750
	0.250	0.750	0.250
	0.750	0.250	0.250

References

Williams, D. B. & Carter, C. B. (1996). *Transmission Electron Microscopy*, pp. 270–275. New York, USA: Springer US.